IEEE Access
Multidisciplinary ⋮ Rapid Review ⋮ Open Access Journal

Received August 29, 2021, accepted September 10, 2021, date of publication September 14, 2021,
date of current version September 28, 2021.

Digital Object Identifier 10.1109/ACCESS.2021.3112885

Comparison of Basic Frequency Selective Surface Design Methods for Optical Windows

İLKER GÜNAY[1,2], TOLGA YELBOĞA[1], YUNUS ÇAT[1], HACI BATMAN[1], AND ASIM EGEMEN YILMAZ[2]

[1]Aselsan Inc., Yenimahalle, 06200 Ankara, Turkey
[2]Department of Electrical and Electronics Engineering, Ankara University, Gölbaşı, 06080 Ankara, Turkey

Corresponding author: İlker Günay (igunay@aselsan.com.tr)

This work was supported by Aselsan Inc.

ABSTRACT Methods for designing frequency selective surface for optical windows are analyzed and experimentally verified. Four methods; ITO coatings, graphene, metallic nano-coatings and metallic meshes; are compared in terms of optical transmission and shielding effectiveness (SE) characteristics. ITO is the most common method for increasing SE performance in the visible band. However, in the infrared band, transmission of ITO is limited. Metallic nano-coating is an alternative for ITO with underperformance from the SE and optical transmission point. Graphene is an emerging method and needs further development. SE performance of the graphene prevents it from being a single material for shielding applications. On the other hand, it might be involved in applications where back reflection is critical because of the electromagnetic absorption characteristic. Metallic mesh is a successful candidate for applications requiring high level SE and optical transmission. However, dielectric properties of substrate the mesh applied, and diffraction effects should be carefully analyzed.

INDEX TERMS Frequency selective surface, ITO, metallic mesh, nano-coating, shielding effectiveness.

I. INTRODUCTION

Imaging systems are being used in more platforms under challenging environmental conditions. It is an essential part of unmanned systems, which are in high demand nowadays. One of the biggest disadvantages of these systems, which have many applications from visible to infrared wavelength, is susceptibility to environmental effects due to their optical windows. These systems, performing surveillance and countermeasure tasks in addition to attacking functions such as searching, tracking, marking, and imaging in the infrared band, are expected to work without any weakness. It is required to be robust against electromagnetic energy generated by RF transmitters. Under these circumstances, optical windows are expected to behave as frequency selective surfaces, meaning that transparent in a wide spectrum from infrared to visible wavelength and filter the microwave frequency band where electromagnetic signals are used frequently.

The associate editor coordinating the review of this manuscript and approving it for publication was Wen-Sheng Zhao.

II. SHIELDING EFFECTIVENESS

Shielding effectiveness (SE) is defined as the ratio of incident field to transmitted field. In other words, reduction of field intensity by reflections and/or losses [20]. The field can be either electric or magnetic field. Shielding effectiveness consists of mainly two terms as absorption and reflection.

The correction factor arises in the case of multiple reflections and can be neglected in plane wave approach [11].

To define absorption loss, another term, skin depth, should be mentioned. The skin depth is explained as the distance required for the electromagnetic wave to attenuate up to 1/e or 37% and expressed as follows:

$$\delta = \sqrt{\frac{2}{\omega\mu\sigma}} \tag{1}$$

Absorption loss occurs as a result of the heating of the environment by resisting currents induced on the surface. The absorption effect for good conductors with thickness t can be expressed as [21]:

$$A = 20\log e^{t/\delta} \tag{2}$$

FIGURE 1. Ultraviolet, visible and infrared spectrum.

Gold is one of the favorite metals for nanoelectronics applications because of its stability and uniformly distributed conductivity. As seen from Figure 2, skin depth of gold is above 500nm up to 18GHz. The thickness of the coating used for most of the lithography applications is less than 300nm and 4nm for ultrathin metallic coatings. Additionally, the lithography process requires evaporation of gold. Gathered gold on the surface has 33% of bulk gold conductivity, which is inversely proportional with skin depth. In light of this information, the thickness of metallic coatings is not sufficient for absorption loss and could be ignored.

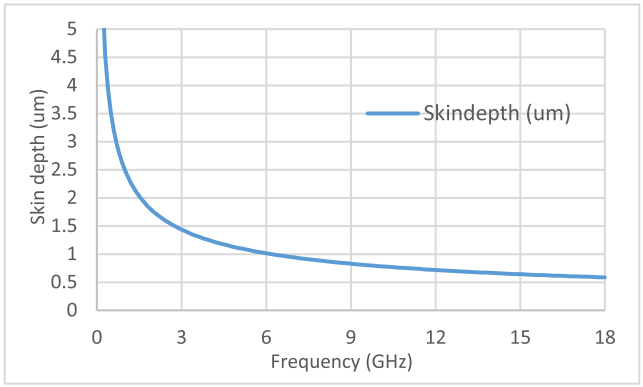

FIGURE 2. Skin depth of gold vs frequency.

The last term, reflection loss, is a function of impedances of incident wave and conductive coating. For a plane wave assumption, the impedance of the incident wave becomes:

$$Z_0 = \sqrt{\frac{\mu_0}{\varepsilon_0}} \tag{3}$$

SE of a conductive coating could be calculated by the ratio of the impedance of the coating to the impedance of the electromagnetic wave [10]:

$$SE(\text{dB}) = 20\log\frac{|Z_{coating}|}{|Z_{wave} + Z_{coating}|} \tag{4}$$

Impedance of the coating consists of real and imaginary parts. While the real part corresponds to the resistance of the coating, the imaginary part represents the reactance. According to transmission line theory, when the thickness of film is less than skin depth δ, the DC resistance of a smooth and continuous metal film coating could be calculated as follows [12]:

$$R_{DC\_coating} = \frac{1}{\sigma t} \tag{5}$$

σ represents the conductivity of the metal and t represents the thickness of the metal. However, the approximation fails when the thickness is less than mean free electron path. This subject will be explained in the following paragraphs.

RF attenuation related to metallic coatings is independent of frequency and could be expressed by the surface resistivity of the coating only [21]. In other words, by using only the resistance of the coating, the RF attenuation can be calculated, and the reactance part can be neglected. In the applications section, formulas and approximations given above will be used when necessary.

III. APPLICATIONS

Evaluating the previous studies, 3 candidate methods have been determined for designing frequency selective optical window. These methods are:''

ITO coatings
Graphene coatings
Metallic Nano Structures.

The concepts of optical transmittance and shielding effectiveness are inversely proportional to each other due to physical nature. In order to increase shielding effectiveness (with same method and feature parameter assumption), optical transmittance should be waived. 3 candidate methods mentioned above will be compared according to shielding effectiveness and optical transmittance performances.

A. ITO COATINGS

First Indium Tin Oxide (ITO) related patent was filed in 1947 making it a mature technology nowadays [16]. ITO coating, which is a member of the metal oxides family, is transparent due to its wide band gaps and has a conductive structure due to the donor level being close to the conduction band [1]. Although these coatings, obtained from the combination of Indium oxide (In_2O_3) and tin oxide (SnO_2), are transparent in the visible band, they act reflective in the infrared band [2].

To examine the performance of ITO, B270 substrate is coated as shown in Figure 3 and tested in terms of optical transparency, SE properties. The optical transmission of uncoated and 360nm thick ITO coated B270 substrate is measured via spectrometer and results are given in Figure 4. In the visible band, transmission of the ITO coating is 93% maximum and 84% average. After a dip around 650nm,

FIGURE 3. ITO coated B270 (left) and 4nm silver coated M-ZnS (right) with uncoated substrates.

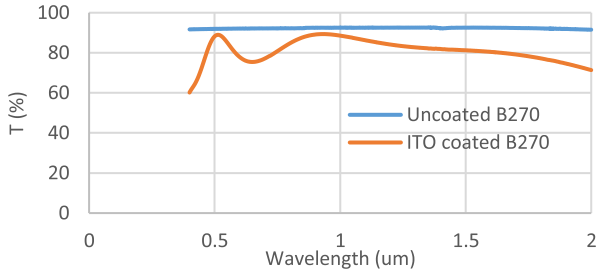

FIGURE 4. Optical transparency of ITO coating.

transmission reaches 86% at 700nm and starts to decrease. After 2000nm, the transparency of ITO is fairly low for optical applications. Anti-reflective coatings can increase the optical performance of ITO especially in the visible band at the expense of increased complexity and the cost.

Sheet resistance of the coating is measured as 23Ω/□ via four-point probe method. Uniformity of the coating is verified by multiple measurements from various locations. Expected theoretical SE value can be calculated as 19.27dB via general SE formula:

$$SE_{DC\_coating} = 20log\left[\frac{1}{1+\frac{Z_0}{2R_{DC\_coating}}}\right] \quad (6)$$

FIGURE 5. PerkinElmer lambda 950 UV/VIS spectrometer setup.

The shielding effectiveness measurement test setup is shown in Figure 7. Shielding effectiveness is measured in 300MHz - 18GHz frequency band via coaxial holder method (details of this method is given in ASTM D 4935 standard and [17]). Vector Network Analyzer (VNA) is used in the setup. 10 successive measurements are taken, and Monte Carlo method is used to eliminate the effects regarding the uncertainties of the measurement system.

ITO coating specified above has shown an average of 18.7dB and a minimum of 16.4dB shielding. The theoretical results and measurement results are close to each other with maximum of 2.9dB deviation.

B. GRAPHENE

Graphene applications have been intensely researched and analyzed in recent years. Although there is still room for improvement in production, transfer from one surface to another and endurance to harsh environmental conditions, deem it worth of investigation due to their promise for characteristics. Based on the research, graphene film's surface resistance performance could be as low as 11Ω/□ with optical transparency of 91% [3]. The current sheet resistance and shielding effectiveness (in the frequency band of 2.2 – 7.5GHz) level of graphene is reported as 635Ω/□ and 2.27dB respectively [14]. Regardless of highest possible performance or current production problems, graphene is not expected to be the single material for shielding applications. However, since most of the SE of graphene originates from absorbance [4], it might be involved in applications where back reflection is critical.

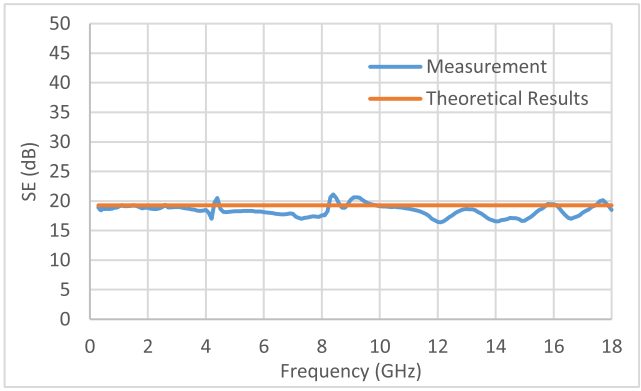

FIGURE 6. Shielding effectiveness results of ITO coating.

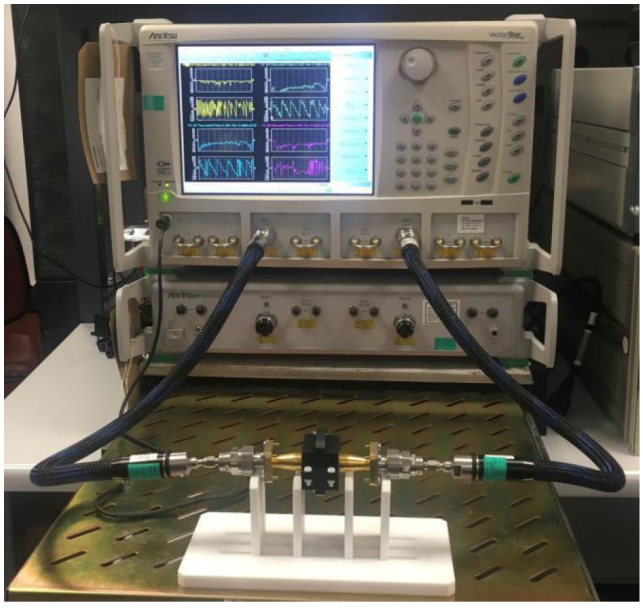

FIGURE 7. Coaxial holder and VNA setup for measurement of SE.

C. METALLIC NANO STRUCTURES

Metals are the best conductive materials on the earth due to their free electron density capacity with high optical opacity. One of the known methods for making metals transparent is

ultrathin coating. Metals can be transparent when the coating thickness is 10nm or less [15]. However, the resistance of metal films increases dramatically when the thickness becomes less than mean free path length. The main reason of this phenomenon is explained as electron scattering at the outer surface and at the crystal boundary [5]. The contribution of additional resistivity in models depends on the bulk resistivity, the mean free path from electron phonon scattering, and the corresponding length scale. Metal with the lowest bulk resistivity and average free path length product ($\rho_0 \times \lambda$) is the most suitable choice for ultrathin structures [6]. Some conductors and their properties are specified in Table 1. Accordingly, although silver is the best conductor in the table, indium, whose resistivity is 5 times higher, has better performance for ultrathin structures.

TABLE 1. Ultrathin performance of some metals [6].

Element	Crystal Structure	$\rho_{0,rt}$ ($\mu\Omega$ cm)	Λ_{rt} (nm)	$\lambda \times \rho_0$ (10^{-14} Ωm^2)
Silver (Ag)	fcc	1.587	53.3	8.46
Copper (Cu)	fcc	1.678	39.9	6.04
Gold (Au)	fcc	2.214	37.7	8.35
Aluminum (Al)	fcc	2.650	18.9	5.01
Indium (In)	bct	8.8	8.65/8.16	7.62/7.18

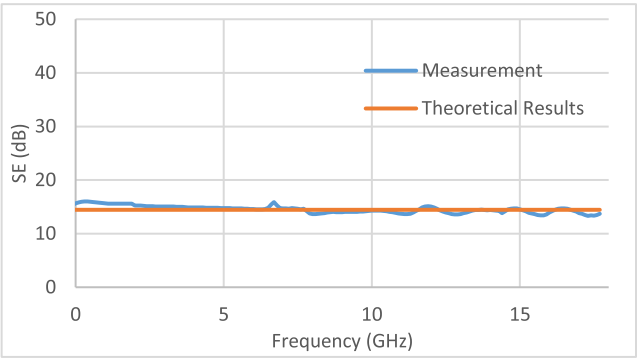

FIGURE 8. Insertion loss results of 4nm silver coated M-ZnS.

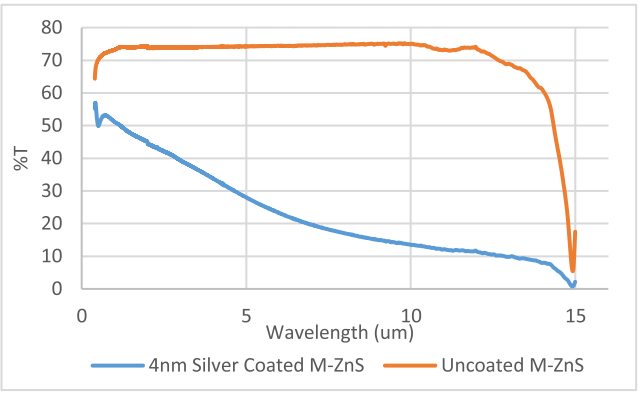

FIGURE 9. Optical transmission results of uncoated and silver coated M-ZnS.

Ultrathin metallic films can provide sufficient optical transmittance for some applications. Although it causes higher reflection in the infrared band, 4nm silver coating is applied on Multispectral ZnS (zinc sulfide) substrate as given in Figure 3. Since silver is an easily oxidizing material, measurements were taken immediately after coating process. The DC resistance of the coating was measured as 44Ω. Expected shielding under these circumstances is 14.5dB according to Eq. (7).

Measurement results given in Figure 8 show that ultrathin silver coating provides approximately 14dB shielding. Expected and measured values are compatible except the 8.5GHz neighborhood.

The optical transmission of the silver coating in nano thickness is shown in Figure 9. Although an average of 75% optical transmittance is achieved in the visible band, the transmittance decreases rapidly in the infrared band. Especially after 7um, optical transmittance decreases to 20% and less which is not an acceptable value.

Another method for designing optically transparent metallic structures is metal mesh with various patterns. The spaces of the mesh provide 100% transmission in the optical spectrum while metal mesh blocks electromagnetic wave. Metal meshes are one of the best candidates when high shielding effectiveness and high optical transmission is required. However, metallic mesh structures behave like a diffraction grating at optical wavelengths and form diffraction order [7].

Diffraction should be considered carefully when mesh size is comparable with the interested optical band. Imaging applications analyze only the central diffraction order (direct incident light) and other diffraction orders have negative effects such as increased background stray light level and reduction in the modulation transfer function (MTF) [7]. Therefore, minimum obscuration is required on the optical window which is inversely proportional with the shielding effectiveness performance.

The advantage of metallic mesh in terms of surface endurance, ease of application and high shielding effectiveness has led to research in detail. It was firstly discussed by Marcuvitz under the topic of microwave-optic elements and tried to be analyzed using transmission line model [8]. Ulrich has taken a step forward with a derived formula semi-empirically for inductive strips, grids and capacitive counterparts [9]. Ulrich stated that an inductive grid behaves as inductive strips when the wavelength is bigger than period of grid ($\lambda \gg g$). However, at resonance frequency, $\lambda = g$, SE will be zero and grid will be completely transparent. To encounter this effect, capacitor is added to equivalent circuit model via experimental validation. Beyond the resonance frequency, Floquet Port analysis gives closer results to measurement

results [22]. However, in most of the applications, resonance frequency is far away and Ulrich method gives reasonable outcomes. Therefore, Ulrich Method is chosen as comparison criteria in the analysis of mesh structures. Although the reactance part of the Ulrich's formula gives quite successful results, the resistance part of the model improved in the succeeding years. First approach was modifying the surface resistance of metallic coatings with correction factors depending on the grid structure [13].

$$R_{DC\_grid} = \frac{1}{\sigma t}\frac{g}{2a} \tag{7}$$

g: period of grid.
2a: width of grid.

Grid resistance formula given in Eq. (7) is quite successful at DC resistance however the frequency dependency is not included. Frequency is added as a variable to resistance model via skin depth by keeping the thickness effect as follows [10]:

$$R_{R_{DC\_grid\_modified}} = \frac{1}{\sigma\delta(1-e^{-t/\delta})}\frac{g}{2a} \tag{8}$$

In the case where the frequency converges to zero, Eq. (8) is equal to Eq. (7). Frequency dependent resistance model used in this study to get more general and comprehensive results.

Ulrich's experimentally validated reactance model [9] for grid structure is used in the calculation of reactance part in this study.

$$X_{Grid} = Z_0\frac{-g}{\lambda}[\ln(sin\frac{\pi a}{g})] \tag{9}$$

Change of skin depth of gold with respect to frequency is given in Figure 2. In photolithography process, gold is evaporated and gathered on the surface of the substrate. However, gathered gold's conductivity is less than bulk gold conductivity level (measured as 1/3) which shows up as decrease at skin depth and SE. The thickness of the coating is approximately 300nm, which is less than 1000nm at 18GHz. Consequently, absorption loss is not considered in the SE calculations. The reflection loss of the grids could be expressed by the formula below:

$$SE = 20log_{10}(\frac{R_{Grid}+iX_{Grid}}{Z_0+R_{Grid}+iX_{Grid}}) \tag{10}$$

Z_0: Free Space Impedance

Photolithography is a process of drawing geometric patterns on the material using light sensitive chemical photoresists. Generally, micro and nanoscale patterns are used and applied to small-scale objects. Since the dimensions of the samples that can be produced (due to infrastructure) cannot be very large, the coaxial holder specified in the ASTM D 4935 standard was preferred as the SE measurement method.

CST MWS Floquet Mode approach is used in order to compare the actual measurements and the analysis method results suggested by Ulrich. CST Floquet Mode approach assumes a single grid structure repeated periodically in an infinitely long plane. Measurements, Ulrich Model and Floquet Port analysis results are shown in Figure 11, Figure 12 and Figure *13*. Accordingly, all results are closely compatible with each other. Reduction of conductivity because

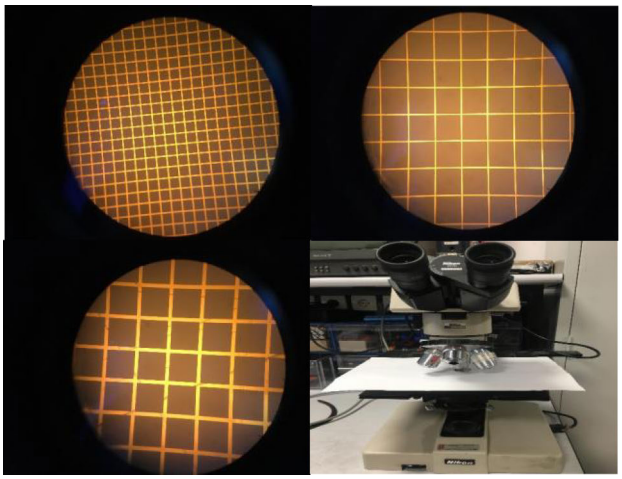

FIGURE 10. Grid geometries of samples (upper left: B1, upper right B3, bottom left B4, bottom right imaging system).

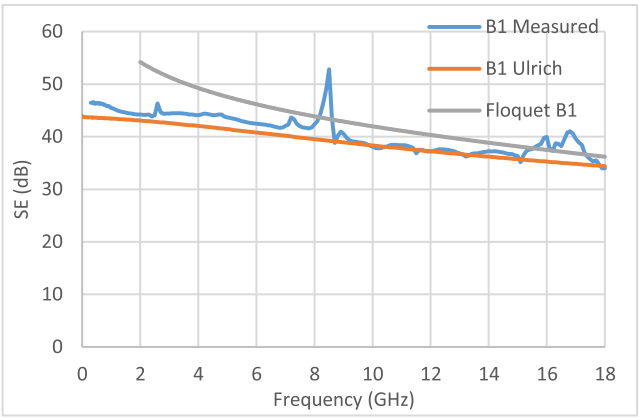

FIGURE 11. B1 grid theoretical and measurement results comparison.

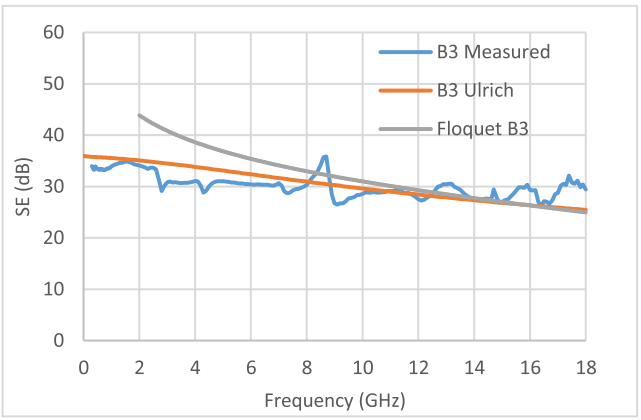

FIGURE 12. B3 grid theoretical and measurement results comparison.

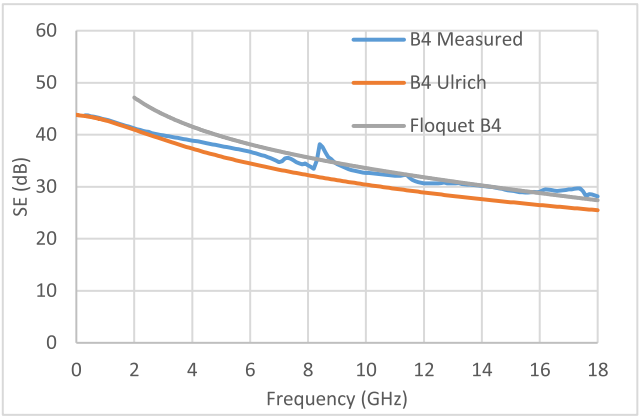

FIGURE 13. B4 grid theoretical and measurement results comparison.

of evaporation and dielectric effects of BK7 substrate are included in Ulrich Method and Floquet Mode analysis.

The waveguide model for the grid structure defined by Marcuvitz [3] and Ulrich [4] as an inductive grid, proves itself as a successful model according to the results stated in this document. According to this model, both resistance and reactance are defined depending on the frequency and the margin of error at high frequencies is reduced. Although the reactance value seems to be ineffective at low frequencies, it becomes the dominant parameter as the frequency increases. The period (g) and line thickness (2a) values of the grid structure appear as the most important parameters affecting the reactance as stated by Ulrich. To emphasize this B1 and B4 samples could be analyzed. Both samples have the same optical obscuration as seen from Table 2 with approximately 10dB SE difference. The reason behind this fact is presented by the Eq.s (8) and (9). The DC resistance of the grids B1 and B4 are equal as shown in Figure 14. However, reactance part of the grids differs by factor 3 which is an outcome of ratio of linewidths of grids. With constant SE requirement, decreasing linewidth causes a decrease at optical obscuration. On the other hand, the decrease in linewidth criteria comes with complex manufacturing techniques which is a drawback issue.

TABLE 2. Properties of the sample.

Samples	Width (um)	Period (um)	Obscuration (%)
B1	5	50	20
B3	5	125	8
B4	15	150	20

Figure 15 shows the variation of line width and optical obscuration parameters to create minimum 15dB SE up to 18GHz. Since the SE is fixed, two-dimensional graph is sketched by calculating the optical obscuration using the period corresponding to the linewidth via Ulrich Method. As the line width decreases, the optical obscuration

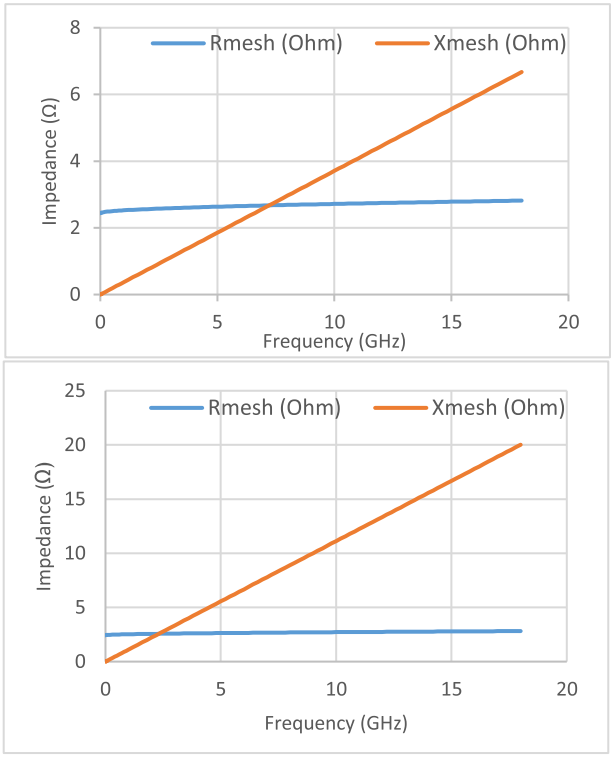

FIGURE 14. Impedance change of B1 (5um/ 50um) (top) and B4 (15um/150um) (bottom) grids.

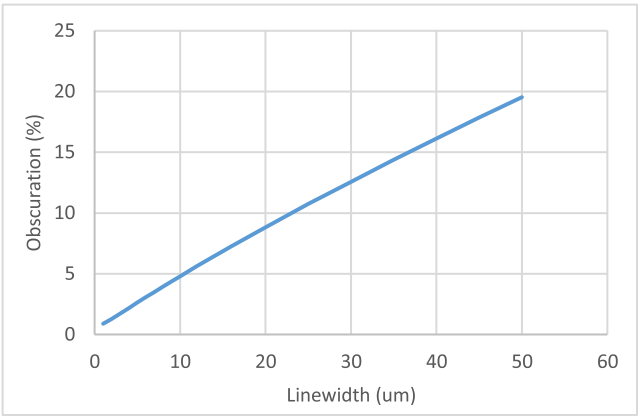

FIGURE 15. Optical obscuration and linewidth change of grids providing 15dB SE up to 18GHz.

decreases. Metallic patterns stand out as the most serious candidates in applications requiring high shielding effectiveness and high optical transmission.

Despite the simplicity of the free-standing grid analysis, in real life, grids will be applied on substrates with various dielectric properties. Optical applications require transparent substrates such as BK7, quartz, sapphire, germanium, ZnS (cleartran) etc. These materials have high relative dielectric constants (sapphire: 11.4, germanium: 16, ZnS: 8.9) which directly affects resonance frequency and the SE performance of the metallic mesh pattern applied. A grid in free space starts

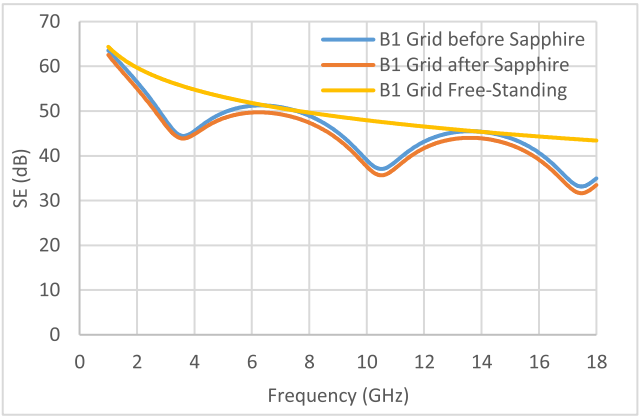

FIGURE 16. Effect of 6.35mm thick sapphire on the SE.

TABLE 3. Comparison of frequency selective optical window design method.

Method	SE (dB)	OT (%)	Transparent Band
ITO	18.7	84	Visible Band
Graphene [14] [23]	2.27	97.7	Broadband
Nano-Coating	14.45	75	Visible Band
Mesh	36 (@18GHz)	80	Broadband

to propagate when the grid period equals to wavelength. This phenomenon is called Wood's Anomaly and the frequency is called resonance frequency [18]. When a dielectric material added in the analysis, the resonance frequency tends to decrease because of the trapped waves in dielectric material [19]. Change of resonance frequency with dielectric existence is shown in Figure 16. To emphasize the substrate effect on grid performance, B1 grid is analyzed free-standing and on 6.35mm sapphire. The period of the free-standing grid causes resonance at 12THz. Up to resonance frequency, SE has a decreasing trend. However sapphire substrate effect shows up as resonance dips at 3.5GHz, 10.5GHz and 17.5GHz. When the material thickness is twice the wavelength, the shielding effectiveness performance approaches the results of analysis performed stand alone.

IV. CONCLUSION

ITO coatings, graphene, metallic nano-coatings and metallic mesh structures are compared in terms of optical transparency and SE parameters. All analysis results are summarized in Table 3. Graphene is a promising method for absorption applications. However, current studies specify minimal effect on SE [23] and cannot be used as a single material for this purpose. Metallic nano-coatings cause a decrease of 4 of optical transmission with 14.45dB SE. Applications require moderate SE and optical transmission is preferable for nano-coatings. On the other hand, ITO has better performance than both graphene and nano-coatings. 16% OT loss at visible band and 1000nm wavelength neighborhood provide 19.27dB SE which is sufficient for most of the frequency selective optical window applications. The popularity of ITO is related to its efficiency and applicability. Metallic mesh structures are the best candidate for applications require high SE and OT values. 36dB SE could be provided with only 5% OT loss. However, measured substrates performed 36dB SE with 20% OT loss and added to comparison as such. Drawbacks of the method such as MTF decrease, dielectric and diffraction effects require careful analysis.

REFERENCES

[1] P. P. Edwards, A. Porch, M. O. Jones, D. V. Morgan, and R. M. Perks, "Basic materials physics of transparent conducting oxides," *Dalton Trans.*, vol. 19, no. 19, pp. 2995–3002, 2004, doi: 10.1039/B408864F.

[2] R. A. Taylor, Y. Hewakuruppu, D. DeJarnette, and T. P. Otanicar, "Fabrication and comparison of selective, transparent optics for concentrating solar systems," *Proc. SPIE*, vol. 9559, Sep. 2005, Art. no. 955905.

[3] S. De and J. N. Coleman, "Are there fundamental limitations on the sheet resistance and transmittance of thin graphene films?" *ACS Nano*, vol. 4, no. 5, pp. 2713–2720, May 2010, doi: 10.1021/nn100343f.

[4] Y. Han, Y. Liu, L. Han, J. Lin, and P. Jin, "High-performance hierarchical graphene/metal-mesh film for optically transparent electromagnetic interference shielding," *Carbon*, vol. 115, pp. 34–42, May 2017, doi: 10.1016/j.carbon.2016.12.092.

[5] E. H. Sondheimer, "The mean free path of electrons in metals," *Adv. Phys.*, vol. 1, no. 1, pp. 1–42, Jan. 1952.

[6] D. Gall, "Electron mean free path in elemental metals," *J. Appl. Phys.*, vol. 119, no. 8, Feb. 2016, Art. no. 085101, doi: 10.1063/1.4942216.

[7] M. Kohin, S. J. Wein, J. D. Traylor, R. C. Chase, and J. E. Chapman, "Analysis and design of transparent conductive coatings and filters," *Proc. SPIE*, vol. 32, no. 5, pp. 911–925, May 1993, doi: 10.1117/12.130266.

[8] N. Marcuvitz, *Waveguide Handbook* (MIT Radiation Laboratory Series). New York, NY, USA: McGraw-Hill, 1951.

[9] R. Ulrich, "Far-infrared properties of metallic mesh and its complementary structure," *Infr. Phys.*, vol. 7, no. 1, pp. 37–55, Mar. 1967, doi: 10.1016/0020-0891(67)90028-0.

[10] Y. Liu and J. Tan, "Frequency dependent model of sheet resistance and effect analysis on shielding effectiveness of transparent conductive mesh coatings," *Prog. Electromagn. Res.*, vol. 140, pp. 353–368, Jun. 2013, doi: 10.2528/PIER13050312.

[11] H. Ott, *Noise Reduction Techniques in Electronic Systems*, 2nd ed. New York, NY, USA: Wiley, 1988.

[12] R. C. Hansen and W. T. Pawlewicz, "Effective conductivity and microwave reflectivity of thin metallic films," *IEEE Trans. Microw. Theory Techn.*, vol. MTT-30, no. 11, pp. 2064–2066, Nov. 1982, doi: 10.1109/TMTT.1982.1131380.

[13] K. T. Jacoby, M. W. Pieratt, J. I. Halman, and K. A. Ramsey, "Predicted and measured EMI shielding effectiveness of a metallic mesh coating on a sapphire window over a broad frequency range," *Proc. SPIE*, vol. 7302, Apr. 2009, Art. no. 73020X1.

[14] S. K. Hong, K. Y. Kim, T. Y. Kim, J. H. Kim, S. W. Park, J. H. Kim, and B. J. Cho, "Electromagnetic interference shielding effectiveness of monolayer graphene," *Nanotechnology*, vol. 23, no. 45, Nov. 2012, Art. no. 455704.

[15] D. S. Ghosh, L. Martinez, S. Giurgola, P. Vergani, and V. Pruneri, "Widely transparent electrodes based on ultrathin metals," *Opt. Lett.*, vol. 34, no. 3, pp. 325–327, Feb. 2009.

[16] D. S. Hecht, L. Hu, and G. Irvin, "Emerging transparent electrodes based on thin films of carbon nanotubes, graphene, and metallic nanostructures," *Adv. Mater.*, vol. 23, no. 13, pp. 1482–1513, 2011.

[17] M. S. Sarto and A. Tamburrano, "Innovative test method for the shielding effectiveness measurement of conductive thin films in a wide frequency range," *IEEE Trans. Electromagn. Compat.*, vol. 48, no. 2, pp. 331–341, May 2006, doi: 10.1109/TEMC.2006.874664.

[18] R. Luebbers and B. Munk, "Some effects of dielectric loading on periodic slot arrays," *IEEE Trans. Antennas Propag.*, vol. AP-26, no. 4, pp. 536–542, Jul. 1978, doi: 10.1109/TAP.1978.1141887.
[19] P. Callaghan, E. A. Parker, and R. J. Langley, "Influence of supporting dielectric layers on the transmission properties of frequency selective surfaces," *IEE Proc. Microw., Antennas Propag. H*, vol. 138, no. 5, pp. 448–454, Oct. 1991.
[20] E. I. Hawthorne, "Electromagnetic shielding with transparent coated glass," *Proc. IRE*, vol. 42, no. 3, pp. 548–553, Mar. 1954, doi: 10.1109/JRPROC.1954.274816.
[21] S. Y. Liao, "Light transmittance and microwave attenuation of a gold-film coating on a plastic substrate (short papers)," *IEEE Trans. Microw. Theory Techn.*, vol. MTT-23, no. 10, pp. 846–849, Oct. 1975, doi: 10.1109/TMTT.1975.1128698.
[22] M. S. Durschlag and T. A. DeTemple, "Far-IR optical properties of free-standing and dielectrically backed metal meshes," *Appl. Opt.*, vol. 20, no. 7, pp. 1245–1253, 1981.
[23] R. R. Nair, P. Blake, A. N. Grigorenko, K. S. Novoselov, T. J. Booth, T. Stauber, N. M. R. Peres, and A. K. Geim, "Fine structure constant defines visual transparency of graphene," *Science*, vol. 320, no. 5881, p. 1308, Jun. 2008.

İLKER GÜNAY received the B.Sc. and M.Sc. degrees in electrical–electronics engineering from Hacettepe University, in 2009 and 2013, respectively. He is currently pursuing the Ph.D. degree in electrical and electronics engineering at Ankara University. He has been working at Aselsan Inc., for 11 years, as an EMC Design Engineer. His research interests include electromagnetic compatibility, EMI filter design, computational electromagnetics, and frequency-selective surfaces.

TOLGA YELBOĞA was born in Istanbul, Turkey, in 1978. He received the B.S. degree in physics engineering from Hacettepe University, in 2001, and the M.S. degree from the Nanotechnology and Nanomedicine Division, Hacettepe University, in 2012.

From 2006 to 2010, he was a Process Engineer with the Bilkent University Nanotechnology Research Center. Since 2010, he has been working as a Process Engineer at Aselsan Inc. His research interests include photolithography, wet etching, plasma etching, PVD coating techniques, flip-chip bonding, and CAD design. He has been designing and fabricating micro-nano structures on different substrates (photodetectors, focal plane arrays, mesh structures, and reticles).

YUNUS ÇAT was born in Ankara, Turkey, in 1989. He received the B.S., M.S., and Ph.D. degrees from the Physic Department, Gazi University, in 2011, 2014, and 2019, respectively.

He is currently working at Aselsan MGEO, Ankara. From 2017 to 2019, he was an Optical Production Engineer with Aselsan Sivas Corporation. His research interests includes the development of bulk crystal (Ge, sapphire) growth, optical window production, AR coating and transparent heaters, and EMI shielding with the fabrication of microstructures.

HACI BATMAN was born in Istanbul, Turkey, in 1978. He received the B.S. degree in engineering physics from the University of Hacettepe, Ankara, in 2001.

He has been an Optical Coating Design and Process Engineer at ASELSAN Inc., since 2003. His research interests include LIDT coatings, different types of optical filters from UV to MWIR band, DLC coatings, and low-reflectance MWIR coatings and metallic coatings.

ASIM EGEMEN YILMAZ received the B.Sc., M.Sc., and Ph.D. degrees in electrical–electronics engineering and mathematics from Middle East Technical University, in 1997, 2000, and 2007, respectively. He is currently with the Department of Electrical–Electronics Engineering, Ankara University, where he is a Professor. His research interests include computational electromagnetics, nature-inspired optimization algorithms, knowledge-based systems, more generally software development processes, and methodologies.